ELSEVIER

Nuclear Physics A581 (1995) 205–219

NUCLEAR PHYSICS A

The Gamow–Teller decay of ^{105}Sn to three-particle states in ^{105}In

M. Pfützner [a], A. Płochocki [a], K. Rykaczewski [a], J. Szerypo [a], J. Żylicz [a], H. Keller [b], R. Kirchner [b], O. Klepper [b], E. Roeckl [b], D. Schardt [b], M. Huyse [c], G. Reusen [c], P. Van Duppen [c], B.A. Brown [d]

[a] *Institute of Experimental Physics, Warsaw University, Warsaw, Poland*
[b] *GSI Darmstadt, Germany*
[c] *Insituut voor Kern- en Stralingsfysika, Leuven, Belgium*
[d] *NSCL and Department of Physics and Astronomy MSU, East Lansing, MI 48823, USA*

Received 12 April 1994; revised 14 June 1994

Abstract

The EC/β^+ decay of ^{105}Sn was reinvestigated by using ^{58}Ni(5 MeV/u) + ^{50}Cr reactions, chemically selective on-line mass separation and γ-ray spectroscopy. The half-life of ^{105}Sn has been determined as 34 ± 1 s. Out of 104 γ transitions ascribed to the ^{105}Sn decay, 89 have been placed in the decay scheme including 52 excited states of ^{105}In. From the EC/β^+ feeding of individual states, the distribution of the Gamow–Teller (GT) strength has been derived. It is shown that the main part of the GT strength is associated with the feeding of ^{105}In levels having excitation energies above 3 MeV. This observation can be interpreted as a sign of dominant feeding of three-quasiparticle states in ^{105}In, which correspond to the $\pi(g_{9/2})^{-1}\nu g_{7/2}\nu d_{5/2}$ shell-model configuration spread over many levels. The sum of the GT strength deduced from the present gamma-ray data of $B_\Sigma(\mathrm{GT}) = 1.46$ provides a lower limit to the total GT strength. Many weak transitions, mainly from high-energy levels, may not have been detected in this study and therefore part of the strength may be missed. An indirect support for this conclusion has been obtained from the analysis of the indium KX-rays intensity. This analysis indicates about 50% contribution of the electron-capture to the beta decay of ^{105}Sn, which is interpreted as a sign of a predominant feeding of the high-energy ^{105}In states with $B_\Sigma(\mathrm{GT}) \geqslant 3$. The observed GT distribution and strength will be compared to results obtained from a finite-Fermi-system theory and a large-basis shell-model calculation. The core-polarization and higher-order hindrance factors will be discussed.

SSDI 0375-9474(94)00330-0

Keywords: RADIOACTIVITY ^{105}Sn (EC), (β^+) [from ^{50}Cr(^{50}Ni, n2p), E = 5.3 MeV/nucleon, mass separation]; measured E_γ, I_γ, $\gamma\gamma$-coin, $T_{1/2}$. ^{105}In deduced levels, Gamow–Teller transition-strength distribution. Enriched target. Ge detectors.
NUCLEAR STRUCTURE ^{105}Sn, ^{105}In; calculated Gamow–Teller transition-strength distribution. Shell model.

1. Introduction

The 31 s EC/β^+ activity of ^{105}Sn was identified at GSI several years ago via the observation of β-delayed protons [1]. Four levels of ^{105}In fed in the ^{105}Sn decay were established later at the LISOL facility [2]. Our intention has been to contribute to studies on the Gamow–Teller (GT) β-decay and on the structure of nuclei near the doubly-magic ^{100}Sn (see Ref. [3]) by reinvestigation the ^{105}Sn EC/β^+ decay scheme.

Spins and parities of the ^{105}Sn and ^{105}In ground states and the 674 keV ^{105m}In isomer are likely to be $\frac{5}{2}^+$ [2,4], $\frac{9}{2}^+$ [5,6] and $\frac{1}{2}^-$ [5], respectively. Within the extreme single-particle shell model (ESPSM), the relevant neutron-particle and proton-hole states are $\nu d_{5/2}$, $\pi(g_{9/2})^{-1}$ and $\pi(p_{1/2})^{-1}$. A direct ^{105}Sn decay to the ground state of ^{105}In is second forbidden and a decay to the isomeric state is first forbidden unique. Such transitions are very slow. Therefore, one may expect that ^{105}Sn undergoes mainly an allowed proton-to-neutron transformation within the even–even core (^{104}Sn), leading to excited states of ^{105}In.

The allowed β decay of neighbouring even–even nuclei proceeds via the $|0^+\rangle \rightarrow |\pi(g_{9/2})^{-1}\nu g_{7/2}, 1^+\rangle$ GT transitions [3]. The same decay channel is expected for the core of ^{105}Sn. Thus, the states fed in ^{105}In should result from the coupling of the $d_{5/2}$ neutron spectator to the 1^+ core state. Their ESPSM configuration is $|\pi(g_{9/2})^{-1}\nu g_{7/2}\nu d_{5/2}, I^\pi\rangle$ with spin and parity $I^\pi = \frac{3}{2}^+, \frac{5}{2}^+, \frac{7}{2}^+$.

From data on neighbouring even–even nuclei [3] and from theoretical considerations [7,8], the GT strength associated with the ^{105}Sn decay to the considered three-quasi-particle states is expected to be quite large. For a rough estimate of the excitation energy of these states one may take the energy of a broken neutron pair. With the pairing-gap parameter $\Delta \approx 12/\sqrt{A}$ being equal to 1.2 MeV in this region, one expects such states to occur above 2 MeV. A shift of the GT strength to relatively high excitation energies, and a large total strength, are predicted also by the finite-Fermi-system theory [9], as well as by the most complete calculation within the shell-model approach [10] with core-polarization [8] accounted for. These predictions will be confronted with our experimental results.

2. Experimental procedure

The experiment was performed at the GSI mass separator on-line to the UNILAC. The ^{105}Sn activity was produced in the ^{50}Cr(^{58}Ni, 2p1n) reaction, whereas the main isobaric contaminant, the 5 min ^{105}In, was produced in the ^{50}Cr(^{58}Ni, 3p)

reaction. The average intensity of the ^{58}Ni beam on the ^{50}Cr target amounted to 50 particle nA. The energy of the projectiles of originally 5.9 MeV/u was degraded down to 5.3 MeV/u in the 2.1 mg/cm^2 molybdenum target backing. The ^{50}Cr target (3.5 mg/cm^2 thickness, 97% enrichment) was placed together with its backing between two copper sieves of 70% transmission.It was mounted in front of a FEBIAD B2C [11] discharge ion source which contained two catcher foils (1.3 mg/cm^2 niobium and 5.3 mg/cm^2 tantalum). For the normal DC operation mode of this source, the average ^{105}Sn and ^{105}In rates after mass separation were 3×10^3 and 9×10^4 atoms/s, respectively. Since the separation efficiency of the catcher-ion-source system for both ^{105}Sn and ^{105}In is expected to be approximately the same (about 30%), the large rate difference should be mainly due to the relevant difference in the production cross sections. The latter is not reproduced by the HIVAP code [12], which gives the cross sections averaged over the target thickness 11 and 34 mb, respectively.

In order to increase the ratio of the ^{105}Sn to ^{105}In activities, the FEBIAD source was operated in the bunched-beam-release mode [13]. This was possible due to an accumulation pocket as part of the enclosure of the ion source. This pocket was alternately cooled for 36 s and heated for 7 s with 2 s overlap, so that the repetition period was 41 s. During the cooling time, tin was trapped and subsequently released by heating the pocket. The transmission of the reaction products to the tape collector (see below) was controlled by beam shutters in the separator beam lines. Adjusted to the tin-release profile, the shutter was open for the last 3 s of each heating time interval. Compared to the DC operation mode, the overall production rate of ^{105}Sn was reduced by a factor of about 3. However, relative to ^{105}In it was enhanced by a factor of roughly 80. The enhancement was due to the fact that almost all indium activity had been released from the ion source before the tin activity was released in a bunch.

The mass-separated $A = 105$ activities were collected on a transport tape. Every 41 s, right after the end of each 3 s collection time interval, the source was transported to the counting station. The station included three Ge(i) detectors and a particle telescope detector. The telescope facing the source had about 10% efficiency for recording emitted protons. Behind the telescope, a large-volume Ge detector (70% standard efficiency) was placed. On the opposite side of the tape, a high-resolution low-energy germanium (LEGe) detector was located in a close geometry. The third Ge detector (30%) was mounted above the tape, at about 5 cm from the source. The full-energy-peak efficiency of the three γ-detectors reached 7.5%, 18.6% and 1.2%, respectively, at the maximum of the calibration curve. The difference between the overall efficiency of the first and third detector was important for estimating the role of summing effects.

The singles γ-ray spectra were measured in a multispectrum mode with 8 time subgroups of 5 s each. Coincidence data were stored event-by-event by using the GOOSY acquisition system on a VAX computer.

Results of γ-ray studies of ^{105}Sn are presented in this paper while the β-delayed proton data of this decay will be discussed in another paper [14] together with analogous data for neighbouring odd-mass tin isotopes.

3. Gamma-ray data and the decay scheme

The total acquisition time of the ^{105}Sn data amounted to 47.5 h. In the singles spectra, γ-lines from the ^{105}In decay dominate over those from the ^{105}Sn decay. Examples of $\gamma\gamma$-coincidence spectra are shown in Figs. 1 and 2.

The analysis of the singles and coincidence spectra led to a list of γ transitions assigned to the ^{105}Sn β-decay, which is presented in Table 1 together with information on the $\gamma\gamma$-coincidence relationships. This list includes the 674.1 keV transition from the 48 s isomer of ^{105}In [15], and the transitions of 309, 424, 992, 1282 and 1416 keV which were observed in the previous ^{105}Sn decay studies [2]. The remaining ones are new. Numerous γ transitions in ^{105}In have been observed

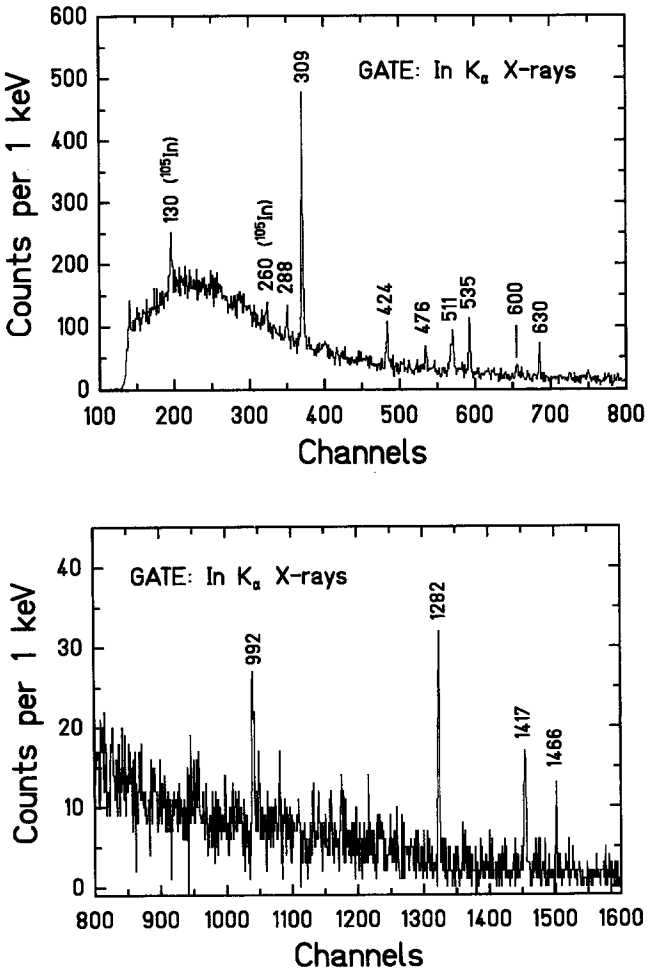

Fig. 1. Gamma spectrum from the 70% Ge detector gated with indium KX-rays. Peak energies are given in keV. Gamma lines from ^{105}In due to random coincidences are indicated.

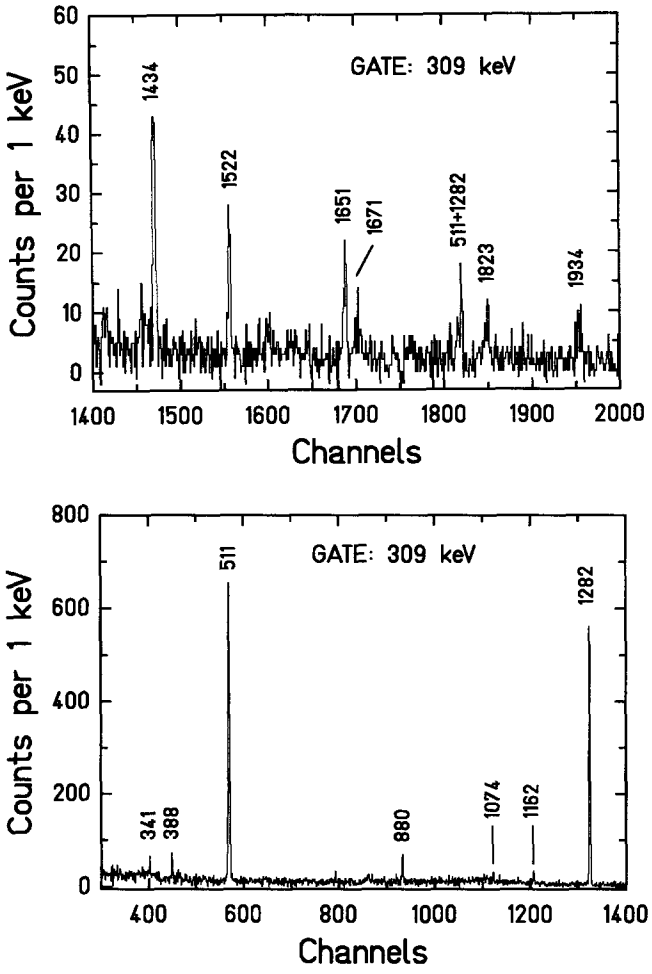

Fig. 2. Gamma lines (recorded in the 70% Ge detector) in coincidence with the 309 keV γ transition in ^{105}In (recorded in the LEGe detector).

in in-beam experiments [16,17]; however, only the 992 keV γ-ray was observed in both β-decay and in-beam work.

For the most intense γ-lines the assignment to the ^{105}Sn decay was established by the observation of a coincidence relation with indium KX-rays. Three of these γ-lines and the indium KX-rays were used for determination of the ^{105}Sn half-life, as illustrated in Fig. 3. The average value from the list-mode data is $T_{1/2} = 34 \pm 1$ s and is confirmed by the multispectrum analysis. The assignment of weaker transitions was additionally based on coincidences with more intense lines already assigned and/or with indium KX-rays. In most cases additional confirmation was supplied by summing relations from the decay scheme.

Table 1
Energies, relative intensities and coincidence relations for γ-rays and indium KX-rays observed in the decay of ^{105}Sn [d]

E_γ (keV)	I_γ^{rel}	Coincident γ-lines
In KX	1571 (40)	see Fig. 1
287.9	21 (4)	629
309.1	289 (6)	341, 388, 880, 1074, 1162, 1282, 1434, 1522, 1651, 1671, 1823, 1934
341.2	16 (8)	309, 1282
388.0	12 (2)	309, 1282
402.1 [a]	9 (1)	903
424.1	78 (4)	954, 992, 2020
476.7	55 (6)	1466, 1651, 1713
535.5	209 (9)	723, 778, 1012, (1060), 1934, 2261
561.7	20 (4)	1417
599.6	36 (4)	1282
628.7	70 (10)	288, 629,1026, 1167
629.3	50 (10)	
674.1	720 [b]	
697.0	24 (14)	1282
722.5	39 (4)	536
733.7 [a]	7 (2)	
756.2	49 (8)	1466
778.3	33 (7)	536
832.3 [a]	< 15	896
880.1	36 (6)	309, 1282
889.9	28 (6)	992
895.7	50 (10)	424, 832, 1417
903.2 [a]	49 (12)	(402) 1466
933.2	48 (4)	1466
954.4	25 (7)	424, 992, 1417
991.8	276 (6)	424, 890, 1434, 1634
1012.4	31 (6)	536
1026.0	17 (2)	629
1040.0	40 (18)	992, 1434, 2426
1046.0	19 (10)	1916
1051.5	26 (11)	1466
1060.2	14 (1)	536
1074.0	11 (6)	309, 1282
1161.5	39 (12)	309, 1282
1167.8	12 (6)	309, 1282
1189.7	22 (6)	1282
1244.5 [c]	34 (6)	
1258.2	66 (1)	
1281.7	1000	309, 388, 600, 820, 880, 1074, 1190, 1434, 1500, 1743, 2190, 2345
1361.9	31 (1)	1916
1364.7	48 (4)	1417
1400.5 [c]	29 (5)	
1415.9	216 (10)	562, 896, 1365
1416.9	231 (10)	
1433.9	45 (7)	309, 992, 1040, 1282
1434.2	25 (4)	
1465.6	553 (20)	477, 756, 933, 1052, 1651, 1693, 1713, 2006, 2190

Table 1 (continued).

E_γ (keV)	I_γ^{rel}	Coincident γ-lines
1477.0	< 10	1282
1486.8	27 (10)	1985
1500.4	53 (7)	1282
1521.7	45 (8)	309, 1282
1547.5	14 (3)	1417
1590.8	35 (8)	
1607.6 [a]	26 (5)	1916
1633.9	29 (5)	992
1651.3	16 (3) + 17 (3)	309, 477, 1282, 1466, 1942
1671.3	21 (4)	309, 1282
1692.5	67 (2)	1466
1713.0	26 (2)	477, 1466
1725.6 [c]	19 (6)	
1742.8	56 (11)	1282
1770.5 [c]	17 (1)	
1822.9	15 (3)	309, 1282
1916.2	149 (9)	1046, 1362, 1608
1934.0	20 (8) + 68 (18)	309, 535, 1282
1942.2	30 (14)	1651
1984.5	139 (12)	1487
2005.9	24 (9)	1466
2019.7 [a]	22 (8)	1417
2108.1	59 (5)	
2120.4	32 (6)	
2132.5	64 (2)	(1282)
2189.8	28 (3) + 27 (3)	1282, 1466
2219.9	41 (3)	424, (1417)
2261.2	35 (4)	536
2283.6	23 (4)	424, (1417)
2290.3	13 (6)	1282
2291.6 [a]	12 (6)	1282
2311.9	26 (5)	1282
2344.8	27 (5)	1282
2351.3 [c]	26 (6)	
2371 [c]	51 (1)	
2426	33 (6)	
2527 [c]	68 (6)	
2589 [a]	39 (2)	
2676 [c]	16 (2)	
2706 [c]	19 (2)	
2732 [c]	45 (8)	
2953	24 (4)	
2984 [c]	42 (3)	
3254 [c]	16 (8)	
3278	96 (6)	
3466	22 (6)	
3472	33 (6)	

Table 1 (continued).

E_γ (keV)	I_γ^{rel}	Coincident γ-lines
3542 [c]	24 (4)	
3636	14 (3)	
3681 [c]	12 (6)	
3700	29 (5)	
3751 [c]	5 (2)	
3787 [c]	10 (4)	
3819 [c]	10 (8)	

[a] Placed tentatively in the decay scheme.
[b] Gamma-ray intensity deduced from the decay scheme after a correction for internal conversion (M4 transition).
[c] Not placed in the decay scheme.
[d] Absolute intensities per 100 decays are obtained by multiplying I_γ^{rel} by 0.0296.

Fig. 4 shows the decay scheme of ^{105}Sn which accounts for 89 out of 104 transitions, i.e. for 93% of the observed γ-ray intensity, listed in Table 1. Transitions and levels marked in Fig. 4 by the dashed lines were placed tentatively in the decay scheme. The normalization of transition intensities was achieved by assuming that neither the ground state nor the isomer of ^{105}In is fed directly in the ^{105}Sn decay (see Section 1), and that the total intensity of the observed γ transitions leading to these two states amounts to 100%. The intensity of the transitions to the isomer defined the intensity of the 674 keV transition. Small corrections for total conversion coefficients were introduced only for the intense 309 and 674 keV transitions under the assumption of multipolarities M1 (tentative) and M4 [5], respectively. The latter multipolarity assumption yielded the intensity of the 674 keV γ-line given in Table 1.

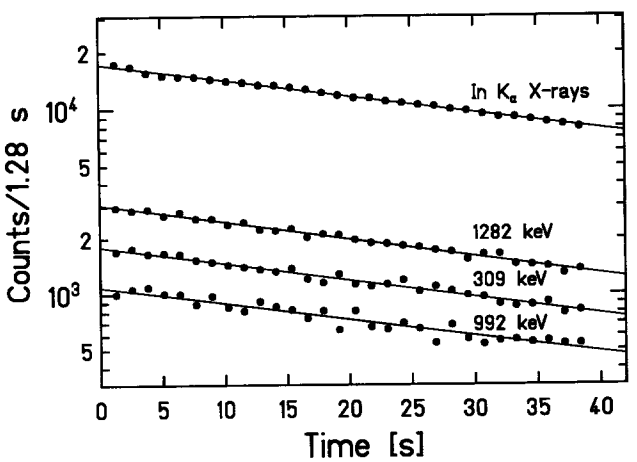

Fig. 3. Determination of the ^{105}Sn half-life. The average value is $T_{1/2} = 34 \pm 1$ s.

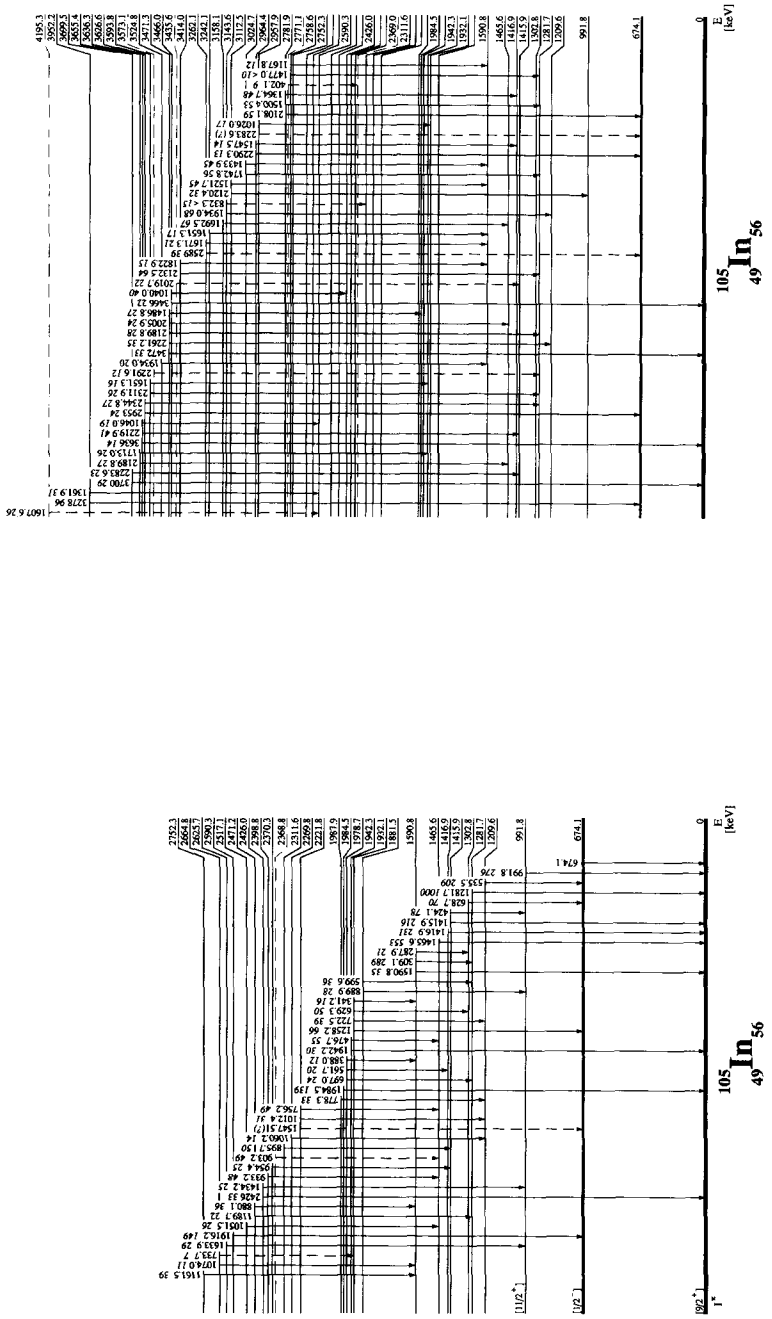

Fig. 4. The decay scheme of ^{105}Sn. Transitions in ^{105}In are marked by their energies (in keV) and their relative intensities. Except for the 309 and 674 keV transitions, intensity corrections for internal conversion have been neglected. Spin and parity assignment are taken from literature (see text).

In a few cases, a transition assigned to the ^{105}Sn decay is accompanied in the spectrum by a transition of nearly the same energy from the ^{105}In decay [5]. The decay pattern is then a sum of short- and long-lived components corresponding to the decay of ^{105}Sn and ^{105}In, respectively. For the lines at 890, 1052 and 1190 keV, the decay-time analysis allowed the extraction of the intensity of the ^{105}Sn component. For the 832, 896, 1477 and 1608 keV transitions this procedure was inconclusive and intensity relations observed in the gated spectra were used to deduce the contribution from ^{105}Sn.

The tentative assignment of the 832 keV transition is based only on the fact that its energy fits to the energy difference of the 3144 and 2312 keV levels. The observed coincidence between the 832 and 896 keV lines cannot be taken as supporting evidence for this assignment because two transitions of these energies are known to be in coincidence also in the decay of ^{105}In.

Gamma lines at 629, 1417, 1434, 1651, 1934 and 2190 keV were identified as doublets and placed twice in the decay scheme. The exact energies of the doublet members were calculated as energy differences of the corresponding levels and the intensities were estimated from coincidence spectra.

There is an ambiguity in placing the 1916 and 1608 keV transitions which were observed to be in coincidence. In Fig. 4 the 1916 keV transition connects the 2590 keV and 674 keV levels while the 1608 keV transition deexcites the level at 4195 keV which is otherwise not confirmed. The position of the level at 2590 keV is supported by the coincidence relation between the 1916 and 1046 keV transitions and by the fact that the latter originates from the well-established level at 3636

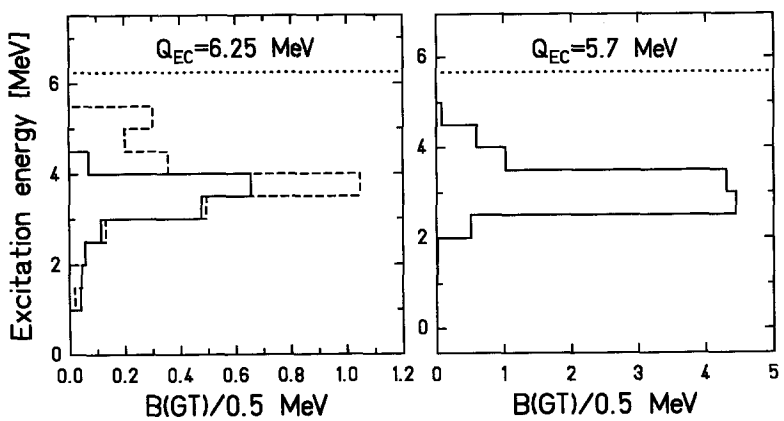

Fig. 5. GT strength per 0.5 MeV for the ^{105}Sn → ^{105}In decay as a function of the excitation energy: (a) Apparent experimental distribution based on the γ-lines place in the decay scheme (solid line); the dashed line shows the distribution obtained under the assumption that γ-lines which are assigned to the decay of ^{105}Sn but not placed in the decay scheme feed levels around 1 MeV; (b) Distribution predicted by the shell model of Ref. [10]. Since the ^{105}In-level energies are calculated relative to the ground-state energy of ^{105}Sn, the latter is taken as a reference for comparison of the theoretical and experimental distributions.

keV. However, the sum 1916 + 1608 keV fits to the energy of the 3524 keV level. It means that the 1916 keV transition may feed the ground state. If the 1916 keV line were a doublet then the position of the 1362 and 3278 keV transitions and of the 3952.3 keV level they deexcite would also be ambiguous.

4. Gamow–Teller strength

4.1. From γ-ray intensities to the GT-strength distribution

Having the total intensities of the gamma transitions one can ascribe the positive difference between the γ-deexcitation intensity and the γ-feeding intensity for each level to the beta feeding of this level. By using the decay energy, $Q_{EC} = 6.25 \pm 0.08$ MeV [18], the corresponding log ft values were calculated and transformed into a distribution of the GT strength via the relation [7]

$$B_i(\mathrm{GT}) = \frac{3862\ \mathrm{s}}{(ft)_i}.$$

The obtained B(GT) distribution is shown in Fig. 5a summed over excitation-energy intervals of 0.5 MeV. The total experimental strength, B_Σ(GT), obtained by summing over all transitions observed, is equal to 1.46 (Table 2).

The distribution in Fig. 5a shows an increase of the GT strength up to excitation energies of 4 MeV and a drastic decrease above. This hints to the fact that a considerable part of the strength associated with high excitations of ^{105}In is missed. Indeed, some distortions of the GT-strength distribution may be connected with the fact that several of the observed lines have not been placed in the decay scheme. Additionally, a large number of transitions from high-energy levels might not have been detected at all (see the discussion of pandemonium in Ref. [19]).

To illustrate a possible role of transitions given in Table 1, which have not been placed in the decay scheme, we assume arbitrarily that they all feed levels around 1

Table 2
Total experimental GT strength of ^{105}Sn (this work) and ^{109}Sn [25] compared with theoretical predictions

Isotope	Q_{EC} (MeV) [18]	B_Σ^{exp}(GT) [a]	B^{th}(GT)	
			FFST [b]	SM [c]
^{105}Sn	6.25	1.46	4.86	4.29
^{109}Sn	3.85	0.82	2.02	–

[a] Derived from the decay scheme and representing a lower limit.
[b] Finite-Fermi-system theory [9].
[c] Shell model of Ref. [10] with an account for core-polarization [8] and higher-order effects [7].

MeV. Under this assumption, the summed strength B_{Σ}(GT) increases to 2.65 and has the distribution shown in Fig. 5a by the dashed line. The unplaced γ-lines, carrying about 7% of the total γ-ray intensity, may thus be responsible for about half of the total GT strength.

4.2. Intensity of KX-rays and the single-level approximation

Predominant feeding of the high-energy states, meaning low EC/β^+ transition energies, should be reflected in a relatively high contribution of the electron capture to the ^{105}Sn decay. To check it we take into account the intensity of indium KX-rays relative to the intensity of γ-rays. From the measured value given in Table 1, after correction for the fluorescence yield, one obtains 54.7 K-shell holes per 100 decays of ^{105}Sn. We estimated that out of this number only 1.3 corresponds to the K-conversion of γ-rays and 53.4 is due to the capture of K electrons. Our expectation of a high EC contribution is thus confirmed.

To get a more quantitative relation between the GT-strength distribution and KX-ray intensity, we can assume that all beta feeding is taken by a single ^{105}In level with energy E_x. Taking the theoretical dependence of the K/(EC + β^+) probability ratio on energy [20], the 53.4% K-capture contribution can be converted to a transition energy of 2.56 MeV. This result together with the Q_{EC} value gives $E_x = 3.69$ MeV. A 100% transition to this state would have log $ft = 3.0$ and B(GT) = 4.2.

It can be shown that a realistic assumption of β-feeding of several states instead of one leads, for a given total K-capture contribution, to a sum of GT strength higher than obtained in the single-level approximation. However, an account for uncertainties in Q_{EC} and in the γ-ray intensities per decay indicates a value of 3 as a safe limit for B(GT).

4.3. Interpretation of the GT strength distribution

In case of ^{105}Sn, we may consider ^{104}Sn as the even–even core. The decay of ^{104}Sn was found experimentally [21] to proceed through GT transitions to four 1^+ levels in ^{104}In with an average excitation energy of 1.4 MeV. This is much lower than the average energy of the GT distribution in the ^{105}Sn decay. Thus, the ESPSM-plus-pairing model predictions given in the introduction are qualitatively supported by our data.

A more advanced approach [9] to a prediction of the GT-strength distribution uses the energy functional method and finite-Fermi-system theory with an account for pairing, particle–hole continuum and effective nucleon–nucleon interaction in particle–hole and particle–particle channels. Also, the influence of higher-order (h.o.) effects is included in a way which is equivalent to introducing a hindrance factor $h_{h.o.} = 1.6$ as, e.g., in Refs. [7,8]. This corresponds to a renormalization of the axial-vector coupling constant such that $|g_A g_V| = 1$ which presumably arises from higher-order configuration mixing and delta-particle nucleon-hole admixtures [22]. The predicted GT strength for the ^{105}Sn → ^{105}In decay is localized at 4.0 MeV

($\approx 94\%$) and 5.6 MeV ($\approx 6\%$). The weighted average of these values is close to the average energy of the experimental GT-strength distribution.

In this approach no estimate is given for the width of the GT-strength distribution. However, the total strength available within the decay-energy window of ^{105}Sn is predicted. As shown in Table 2, the predicted strength is about 3 times larger than the experimental value obtained by summing over all transitions observed. In this context it is worth noticing that the summed experimental strength observed for the decay of ^{104}Sn [21] exceeds that for ^{105}Sn. It amounts to ≈ 2.5, which is about 50% of the value predicted in Ref. [9] for the ^{104}In levels below $Q_{EC} = 4.515$ MeV.

The most complete theoretical picture of the β-decay of ^{105}Sn has been obtained within the shell-model approach [10]. The model space used in the calculations includes $\pi g_{9/2}$, $\pi p_{1/2}$, $\nu g_{7/2}$ and $\nu d_{5/2}$ orbitals. The single-particle energies and two-body matrix elements for protons were calculated with the seniority-conserving interaction of Gloeckner and Serduke [23]. The neutron single-particle energies were determined from experimental data on the states in the odd–even $N = 50$ nuclei. To obtain the relevant two-body matrix elements a modified surface delta interaction was used [24]. The proton–neutron interaction was calculated from the bare G matrix of Hosaka et al. [25] based on the Paris potential. The proton–neutron matrix elements were renormalized by a factor of 0.7 in order to better reproduce the Z dependence of the $g_{7/2}$ and $d_{5/2}$ splitting in the odd–even $N = 51$ nuclei.

The GT strength from these shell-model calculations is distributed over more than 300 transitions from the $\frac{5}{2}^+$ ground state of ^{105}Sn to the $\frac{3}{2}^+$, $\frac{5}{2}^+$ and $\frac{7}{2}^+$ excited states of ^{105}In located at excitation energies between 1 and 5 MeV. As seen in Fig. 5b, the width of the calculated distribution resembles the experimental one.

The sum of the shell-model GT-strength values amounts to 11.0. This number is already smaller than $10 \times \frac{16}{9} \cong 17.8$ given by the ESPSM. The difference is due to the nonzero occupancy of the neutron $g_{7/2}$ orbital in the ^{105}Sn ground state. A further step toward experiment is made by accounting for the core-polarization. The core-polarization (c.p.) hindrance factor estimated in Ref. [8] for ^{100}Sn is $h_{c.p.} = 1.60$. This value may be valid roughly also for heavier tin isotopes. Its application to ^{105}Sn reduces the strength to the value of 6.87. Further application of the hindrance factor $h_{h.o.} = 1.6$ corresponding to higher-order effects reduces the predicted strength to the value 4.29 given in Table 2. The strength derived from the decay scheme is 34% of the calculated value. The total strength in the two theoretical approaches is similar, and both are much larger than the experimental lower limit of 1.46.

To explain the remaining discrepancy one has to refer to the problem of the strength missed in the measurements. If the real experimental strength were above 3, as suggested by our estimates presented in Section 4.2, a good agreement with theory would be possible.

A comparison between the shell-model predictions and the experiment can be performed in a different way which does not depend upon the strength missed in the decay-scheme study. Without an account for the core-polarization and the

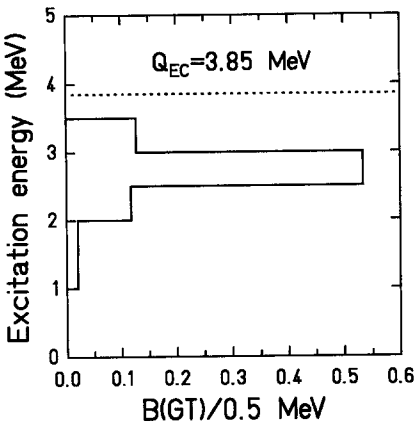

Fig. 6. Experimental GT strength per 0.5 MeV as a function of the excitation energy for the $^{109}Sn \rightarrow {}^{109}In$ decay.

higher-order effects, the shell-model calculation gives $T_{1/2} = 12.9$ s for ^{105}Sn. Multiplication of this value by the hindrance factors $h_{c.p.}$ and $h_{h.o.}$ considered above gives 33 s, which is surprisingly close to the experimental half-life value of 34 ± 1 s.

Fig. 6 and Table 2 contain also information on the distribution and sum of the GT strength for the $^{109}Sn \rightarrow {}^{109}In$ decay. The decay-scheme data have been taken from a recent compilation [26]. Since the ^{109}Sn and ^{109}In ground states are likely to be the $\nu d_{5/2}$ and $\pi(g_{9/2})^{-1}$ shell-model states, the interpretation of the data is quite analogous to that for the ^{105}Sn decay.

5. Summary and conclusions

Our experimental data on the ^{105}Sn decay show that the main part of the GT strength is associated with the feeding of ^{105}In states at excitation energies greater than 3 MeV. This observation is compatible with the simple picture according to which this decay occurs within the even–even core leading to three-quasi-particle states which correspond to the $\pi(g_{9/2})^{-1}\nu g_{7/2}\nu d_{5/2}$ shell-model configuration. It supports also the predictions based on the finite-Fermi-system theory and on a configuration-mixed shell-model. The models predict the total strength essentially higher than the experimental B_Σ(GT) value. Before a final conclusion can be drawn about quenching of the GT strength in this case one has to clarify what fraction of the strength is missed due to the application of the high-resolution but low-efficiency γ-spectroscopy. This could be done by using a total-absorption γ-ray spectrometer. However, it would require a more selective production of ^{105}Sn. An application of the laser ion source [27] could be the appropriate solution for this task.

One of the authors (B.A.B.) would like to acknowledge support from the Alexander von Humboldt foundation and from NSF grant 90-17077. The authors from Warsaw would like to kindly acknowledge a support and hospitality of GSI and a support from the Polish Committee of Scientific Research.

References

[1] P. Tidemand-Petersson, R. Kirchner, O. Klepper, W. Kurcewicz, E. Roeckl and E.F. Zganjar, Z. Phys. A 302 (1981) 343.
[2] K. Deneffe, E. Coenen, M. Huyse, P. Van Duppen, J. Vanhorenbeeck, P. del Marmol and P. Fettweis, J. of Phys. G 11 (1985) L59.
[3] K. Rykaczewski, Proc. 6th Int. Conf. on nuclei far from stability & 9th Int. Conf. on atomic masses and fundamental constants, Bernkastel-Kues 1992, eds. R. Neugart and A. Wöhr (IOP, Bristol, Philadelphia, 1993) p. 517.
[4] R. Schubart, H. Grawe, J. Heese, H. Kluge, K.H. Maier, M. Schramm, J. Grębosz, L. Käubler, H. Rotter, J. Kownacki and D. Seweryniak, Z. Phys. A 343 (1992) 123, and references therein.
[5] J. Verplancke, E. Coenen, K. Cornelis, M. Huyse, G. Lhersonneau and P. Van Duppen, Z. Phys. A 315 (1984) 307.
[6] D. Vandeplassche, E. van Walle, C. Nuytten and L. Vanneste, Phys. Rev. Lett. 49 (1982) 1390.
[7] I.S. Towner, Nucl. Phys. A 444 (1985) 402.
[8] I.P. Johnstone, Phys. Rev. C 44 (1991) 1476.
[9] I.N. Borzov, E.L. Trykov and S.A. Fayans, Proc. 6th Int. Conf. on nuclei far from stability & 9th Int. Conf. on atomic masses and fundamental constants, Bernkastel-Kues 1992, eds. R. Neugart and A. Wöhr (IOP, Bristol, Philadelphia, 1993) p. 651;
I.N. Borzov, S.A. Fayans and K. Rykaczewski, Gamow–Teller β-decay of tin isotopes near ^{100}Sn, to be published.
[10] B.A. Brown and K. Rykaczewski, Gamow–Teller strength in the region of ^{100}Sn, Phys. Rev. C, in print.
[11] R. Kirchner, Nucl. Instr. and Meth. B 26 (1987) 204.
[12] W. Reisdorf, Z. Phys. A 300 (1981) 227; GSI Report GSI 81-2 (1981) 73.
[13] R. Kirchner, O. Klepper, D. Marx, G.-E. Rathke and B. Scherrill, Nucl. Instr. and Meth. A 247 (1986) 265.
[14] Darmstadt–Leuven–Mainz–Troizk–Warsaw Collaboration, to be published.
[15] J. Rivier and R. Moret, Radiochim. Acta **22** (1975) 27.
[16] T. Ishii, A. Makishima, M. Nakajima, M. Ogawa, M. Ishii, Y. Saito and S. Garnsomsart, Z. Phys. A 343 (1992) 261.
[17] D. Seweryniak et al., private communication (1993).
[18] G. Audi and A.H. Wapstra, Nucl. Phys. A 565 (1993) 1.
[19] J.C. Hardy, B. Jonson and P.G. Hansen, Phys. Lett. B 136 (1984) 331.
[20] B.S. Dzhelepov, L.N. Zyrianova and Yu.P. Suslov, Beta processes (Nauka, Leningrad, 1972).
[21] R. Barden, R. Kirchner, O. Klepper, A. Plochocki, G.-E. Rathke, E. Roeckl, K. Rykaczewski, D. Schardt and J. Żylicz, Z. Phys. A 329 (1988) 319.
[22] B.A. Brown and B.H. Wildenthal, Nucl. Phys. A 474 (1987) 290.
[23] D.H. Gloeckner and F.J.D. Serduke, Nucl. Phys. A 220 (1974) 447.
[24] P.W.M. Glaudemans, P.J. Brussaard and B.H. Wildenthal, Nucl. Phys. A 102 (1967) 593.
[25] A. Hosaka, K.I. Kubo and H. Toki, Nucl. Phys. A 444 (1985) 76.
[26] J. Blachot, Nucl. Data Scheets **64** (1991) 913.
[27] F. Sheerer, F. Albus, F. Ames, H.-J. Kluge and N. Trautmann, Spectrochim. Acta, Part B 47 (1992) 793; V.N. Fedoseyev, Y. Jading, R. Kirchner, O. Klepper, H.-J. Kluge, K.-L. Kratz, V.I. Mishin, E. Roeckl, F. Scheerer and K. Schmidt, GSI Science Report 1993 GSI 94-1, (1994).